Author Manuscript

Author Manuscript

Author Manuscript

Author Manuscript

HHS Public Access

Author manuscript

Nature. Author manuscript; available in PMC 2020 January 22.

Published in final edited form as:

Nature. 2019 August ; 572(7769): 387–391. doi:10.1038/s41586-019-1439-1.

Regulation of phosphoribosyl ubiquitination by a calmodulin-dependent glutamylase

Ninghai Gan[1,*], **Xiangkai Zhen**[2,3,*], **Yao Liu**[1,*], **Xiaolong Xu**[2,*], **Chunlin He**[4], **Jiazhang Qiu**[5], **Yancheng Liu**[1], **Grant M. Fujimoto**[6], **Ernesto S. Nakayasu**[6], **Biao Zhou**[2], **Lan Zhao**[2], **Kedar Puvar**[7], **Chittaranjan Das**[7], **Songying Ouyang**[2,3,¶], **Zhao-Qing Luo**[1,¶]

[1]Purdue Institute for Inflammation, Immunology and Infectious Disease and Department of Biological Sciences, Purdue University, West Lafayette, IN 47907, USA

[2]The Key Laboratory of Innate Immune Biology of Fujian Province, Provincial University Key Laboratory of Cellular Stress Response and Metabolic Regulation, Biomedical Research Center of South China, Key Laboratory of OptoElectronic Science and Technology for Medicine of the Ministry of Education, College of Life Sciences, Fujian Normal University, Fuzhou, 350117, China.

[3]Laboratory for Marine Biology and Biotechnology, Pilot National Laboratory for Marine Science and Technology (Qingdao), Qingdao 266237, China.

[4]Key Laboratory of Organ Regeneration and Transplantation of the Ministry of Education, Department of Respiratory Medicine and Center of Infection and Immunity, The First Hospital of Jilin University, Changchun 130021, China

[5]Key Laboratory of Zoonosis, Ministry of Education, College of Veterinary Medicine, Jilin University, Changchun, Jilin 130001, China

[6]Biological Science Division, Pacific Northwest National Laboratory, Richland, WA 99352, USA

[7]Department of Chemistry, Purdue University, West Lafayette, IN 47907, USA

Keywords

Legionella; Type IV secretion; ubiquitin; SdeA; glutamylation; ADP-ribosylation

The bacterial pathogen *Legionella pneumophila* creates an intracellular niche permissive for its replication by extensively modulating host cell functions using hundreds of effector proteins delivered via its Dot/Icm secretion system[1]. Among these, members of the SidE

Users may view, print, copy, and download text and data-mine the content in such documents, for the purposes of academic research, subject always to the full Conditions of use:http://www.nature.com/authors/editorial_policies/license.html#termsReprints and permissions information is available at www.nature.com/reprints.

¶Correspondence: ouyangsy@fjnu.edu.cn, luoz@purdue.edu.
*These authors contributed equally to this work.

Author contributions NG and ZQL conceived the ideas for this work. Unless specified, NG and YL performed the experiments. YL, NG and JQ performed the yeast experiments; GF and ESN performed mass spectrometric analyses. XZ, XX, CH, BZ, LZ and SO determined the structures and analyzed protein properties using biophysical tools. KP and CD performed HPLC analysis of nucleotide products. NG, YL, ESN, SO and ZQL interpreted the results. NG, YL, SO and ZQL wrote the manuscript and all authors provided editorial input.

The authors declare no competing financial interests. Readers are welcome to comment on the online version of the paper.

Supplementary information is available in the online version of the paper.

Author Manuscript Author Manuscript Author Manuscript Author Manuscript

family (SidEs) regulate multiple cellular processes by a unique phosphoribosyl ubiquitination mechanism that bypasses the canonical ubiquitination machinery[2-4]. The activity of SidEs is regulated by SidJ, another Dot/Icm effector[5], but the mechanism of such regulation is not completely understood[6,7]. Here we demonstrate that SidJ inhibits the activity of SidEs by inducing covalent attachment of glutamate moieties to E860 of SdeA, which is one of the catalytic residues for the mono-ADP-ribosyltransferase activity involved in ubiquitin activation[2]. The inhibition by SidJ is spatially restricted in host cells because its activity requires the eukaryote-specific protein calmodulin (CaM). We solved a structure of SidJ-CaM in complex with adenosine monophosphate (AMP) and found that the ATP utilized is cleaved at the α phosphate position by SidJ which in the absence of glutamate or modifiable SdeA undergoes self-AMPylation. Our results reveal an unprecedented mechanism of regulation in bacterial pathogenicity in which a glutamylation reaction that inhibits the activity of virulence factors is activated by host factor-dependent acyl-adenylation.

Ubiquitination regulates many aspects of immunity, pathogens have thus evolved various strategies to co-opt the ubiquitin network to promote their virulence8[8,9]. One such example is the SidE family effectors from *Legionella pneumophila*, which ubiquitinate structurally diverse proteins associated with the endoplasmic reticulum[2,4]. Ubiquitination by SidEs is initiated via ADP-ribosylation at R42 of ubiquitin catalyzed by the mono-ADP ribosyltransferase (mART) activity[2]. The activated ADP-ribosylated ubiquitin (ADPR-Ub) is then utilized by a phosphodiesterase(PDE)-like domain also harbored by SidEs, which ligates phosphoribosylated ubiquitin (PR-Ub) to serine residues of substrate proteins[2,3]. Because both ADPR-Ub and PR-Ub impair the function of eukaryotic cells by inhibiting canonical ubiquitination[3], which is pivotal for bacterial virulence[10], factors of either bacterial or host origin that function to prevent potential cellular damage caused by these molecules likely exist.

The activity of members of the SidE family such as SdeA is regulated by SidJ[5] which suppresses its yeast toxicity[6]. SidJ purified from *L. pneumophila* also appears to remove ubiquitin from modified substrates[7]. Despite these observations, questions about the mechanism of action of SidJ remain. For example, the $SdeA_{H277A}$ mutant defective in the PDE activity still is toxic to yeast but cannot ubiquitinate substrates[3], but whether SidJ can suppress its toxicity is unknown. Furthermore, it is not clear why the deubiquitinase activity is only observed in SidJ purified from *L. pneumophila*[7].

We set out to address these questions by constructing a yeast strain which inducibly expressed $SdeA_{H277A,}$ and found that SidJ effectively suppressed its toxicity (Fig. 1a). Thus, SidJ may neutralize the toxicity of ADPR-Ub or target the ADP-ribosylation activity of SdeA. In addition, SidJ severely reduced protein modification induced by SdeA and effectively relieved SdeA-induced inhibition of the hypoxia-inducible factor 1-α degradation[3] (Fig. 1b-c). However, SidJ purified from *E. coli* or mammalian cells failed to remove ubiquitin from modified proteins nor did it detectably affect SdeA-induced Rab33b ubiquitination (Fig. 1d-e). Together, these results suggest that SidJ affects the function of SdeA but the *in cellulo* activity cannot be recapitulated by biochemical reactions.

Author Manuscript Author Manuscript Author Manuscript Author Manuscript

Differing from Flag-SdeA coexpressed with GFP or the $SidJ_{DD/AA}$ mutant defective in suppressing SdeA yeast toxicity[6] that robustly modified Rab33b, Flag-SdeA obtained from cells coexpressing GFP-SidJ (Flag-SdeA*) failed to ubiquitinate Rab33b (Fig. 2a). We next examined whether SidJ affects the mART activity in reactions that measure the ability of Flag-SdeA* to use ubiquitin or ADPR-Ub for ubiquitination. Flag-SdeA* lost the ability to catalyze ubiquitination from ubiquitin, but retained the ability to use ADPR-Ub for ubiquitination (Fig. 2b). Consistently, Flag-mART ($SdeA_{563–910}$)[11] purified from HEK293T cells expressing GFP-SidJ (Flag-mART*) also failed to ubiquitinate Rab33b with the PDE-competent $SdeA_{E/A}$ mutant[3,4] (Fig. 2c). Thus, SidJ targets the mART activity of SdeA.

Liquid chromatography tandem mass spectrometric (LC-MS/MS) analysis identified a mass shift of 129.04 Da (m/z =129.04, z=1) on the peptide - H_{855}GEGTESEFSVYLPEDVALVPVK$_{877–}$ in Flag-mART* (Fig. 2d-e). The modification, likely by the addition of a glutamate was mapped to E860, one of the catalytic residues for the mART[2] (Fig. 2e). Approximately 93.7% of E860 was modified in samples coexpressed with GFP-SidJ and a modification of 258.09 Da (m/z =258.09, z=1), presumably diglutamate was also detected on a small portion of the same peptide (Extended data Fig. 1). Thus, SidJ may be a glutamylase that ligates one or multiple glutamate moieties to E860 of SdeA.

We did not detect SidJ activity in reactions containing ATP, the energy source for known glutamylases[12] and L-glutamate, or its structural isomers N-acetylserine and N-methyl-aspartate (Extended data Fig. 2a). Because the inhibitory effects of SidJ was evident only when it is expressed in mammalian cells, we tested the hypothesis that its activity requires one or more factors of eukaryotic origin by including lysates of *E. coli* or HEK293T cells in the reactions. Lysates of HEK293T cells (native or boiled) caused a decrease in Rab33b modification (Extended data Fig. 2b), indicating that one or more heat-stable factors specific to eukaryotic cells are required for the activity of SidJ.

Pfam analysis[13] found an IQ-like motif involved in calmodulin (CaM) binding near the carboxyl end of SidJ (Fig. 3a). Yeast toxicity of SidJ[14] was suppressed by mutations in I841 and Q842, two residues in IQ motifs important for CaM-binding[15] or by the yeast CaM gene *cmd1* (Fig. 3b), validating the IQ motif. Indeed, binding between SidJ and CaM occurred in cells infected with relevant *L. pneumophila* strains or coexpressing these two proteins, and the IQ motif is needed for optimal binding (Fig. 3c-d).

CaM, SidJ together with L-glutamate, but not the two glutamate isomers abolished SdeA-mediated ubiquitination (Fig. 3e). Consistent with the heat-insensitivity seen in mammalian cell lysates, boiled CaM was partially active (Extended data Fig. 2c). Importantly, we found that SdeA can be modified by ^{14}C-glutamate only in reactions containing CaM, and that $SdeA_{E860A}$ cannot be modified by ^{14}C-glutamate, establishing that E860 is the major modification site (Fig. 3f). Similar to other glutamylases[12], ATP binds SidJ (K_d=1.45 μM) and is required for SidJ activity (Extended data Fig. 2d-e). CaM-dependent inhibition by SidJ occurred to all SidE family members (Extended data Fig. 2f). Under our experimental conditions, 0.006 and 0.055 μM of CaM was required to activate SidJ and $SidJ_{IQ/DA}$, respectively, which explained the observation that $SidJ_{IQ/DA}$ still complemented the

Author Manuscript Author Manuscript Author Manuscript Author Manuscript

phenotype associated with the *ΔsidJ* mutant (Extended data Fig. 3). Together, these results establish that SidJ is a CaM-dependent glutamylase that catalyzes the ligation of glutamate moieties to E860 of SdeA.

We further probed the mechanism of the CaM-dependent glutamylase activity of SidJ by structural analysis. A SidJ truncation lacking its first 99 residues ($SidJ_{\Delta N99}$) was indistinguishably active compared to full-length protein. Biophysical analysis indicated that it formed a stable heterodimer with CaM at the ratio of 1:1 (Extended data Fig. 4). We solved a 2.71 Å structure of the $SidJ_{\Delta N99}$-CaM complex using a 2.95 Å structure of the $SidJ_{Se\text{-}Met}$-CaM derivative as the search model (Extended data Table 1). Two SidJ-CaM heterodimeric complexes are found in one asymmetric unit (ASU) (Extended data Fig. 5a). Intersubunit contacts analysis in the ASU suggests that the interface between the two SidJ molecules in the structure results from crystal packing. $SidJ_{\Delta N99}$ in the complex folds into three distinct domains which we designated as the N-terminal domain (NTD), the Central domain (CD), and the C-terminal domain (CTD) (Fig. 4a). CaM docks onto the carboxyl end that contains the IQ motif (Fig. 4b). The interface area between SidJ and CaM is about 1574 $Å^2$, which accounts for 17.6% of the surface of CaM.

$SidJ\Delta_{N99}$ interacts extensively with CaM via hydrogen bonds and salt bridges. Specifically, Q830 and Q842 of SidJ engage in hydrogen-bonding interactions with E85 and S102 of the CaM C-lobe, respectively. Other hydrogen bonds include S808(SidJ) and E812(SidJ):R38(CaM), R804(SidJ):S39(CaM), R660(SidJ) and R796(SidJ):E15(CaM) (Fig. 4b). Mutations in these residues reduced the binding affinity of SidJ for CaM (Fig. 4c).

We determined the role of ATP in SidJ activity by crystallizing the $SidJ\Delta_{N99}$-CaM complex in the presence of ATP and obtained a structure to 3.11 Å resolution (Extended data Table 1). We observed an AMP moiety bound in a pocket formed in the CD. This domain along with approximately a hundred additional residues is designated as the kinase domain in a recent study[16], where the same pocket is shown to be occupied by pyrophosphate and Mg^{2+} ions. The AMP moiety, likely a product of ATP breakdown induced by SidJ, is coordinated by R352, K367, Y532, N534, R536 and D545 (Fig. 4d). Ala substitution of R352, K367, N534, R536 or D545 abolished the activity of SidJ, whereas a mutation in the distal Y443 had no effect (Fig. 4e). The binding of AMP does not cause obvious conformational changes in the $SidJ_{\Delta N99}$-CaM complex (Extended data Fig. 5b). In our structures, we observed CaM in a relatively closed conformation[17] with one Ca^{2+} coordinated in the EF1 site of CaM (Extended data Fig. 6a). However, Ca^{2+} in our structures exhibited a relatively high B-factor indicating partial occupancy of the ion, which is consistent with the partial disorder in the CaM polypeptide in the crystals. CaM remained active even after dialysis against EGTA or inclusion of this chelator in the reactions (Extended data Fig. 6b-c).

The presence of AMP in the structure suggests that ATP was cleaved at the α site during reaction. Indeed, ATP analogs adenylyl-imidodiphosphate and ATP-γ-S, which cannot be effectively hydrolyzed at the γ site, still activated SidJ (Fig. 4f). ADP, but not AMP or adenosine, potently induced the activity of SidJ, and ATP-α-S, which can be slowly hydrolyzed at the α-site[18], partially supported SidJ activity. In contrast, ApCpp harboring an

Author Manuscript Author Manuscript Author Manuscript Author Manuscript

uncleavable α-site failed to detectably activate SidJ (Fig. 4g). Thus, the SidJ-catalyzed reaction involves the cleavage of ATP between the α and β phosphates.

SidJ-induced cleavage of ATP is akin to the reaction involved in AMPylation[19], we thus examined whether SidJ catalyzes AMPylation using ^{32}P-α-ATP. Robust self-AMPylation of SidJ was detected in reactions containing CaM; such modification also occurred in glutamylation reactions lacking glutamate or modifiable SdeA (Extended data Fig. 7a-b). Furthermore, residues important for binding AMP are required for the self-modification activity (Fig. 4h). We detected AMP in reactions containing SidJ, CaM and ATP, and the release of AMP was accelerated by SdeA but not $SdeA_{E860A}$ (Extended data Fig. 7c). We propose a model in which SidJ activates E860 of SdeA by acyl-adenylation, which is followed by nucleophilic attack of the amino group of free glutamate on the activated carbonyl of the unstable E860-AMP intermediate, leading to glutamylation of E860 and AMP release (Extended data Fig. 7d).

Overexpression of SdeA in the Δ*sidJ* mutant severely affected intracellular bacterial replication[6,20], so did $SdeA_{ML/AA}$ defective in substrate recognition[11] and such defects can be rescued by simultaneous expression of SidJ (Extended data Fig. 8). We attempted to separate the ubiquitin ligase activity from being the substrate for SidJ by constructing $SdeA_{E860D}$. SidJ can neither modify this mutant nor suppress its yeast toxicity. Similarly, its ubiquitin ligase activity is insensitive to SidJ. Most relevantly, its inhibition of intracellular growth of the Δ*sidJ* strain cannot be rescued by SidJ (Extended data Fig. 9).

The AMP-binding site in our structure is critical for the activation step, but it remains unclear how free Glu is recognized. The E860-AMP intermediate produced at this site may transit to a second nucleotide-binding site in the same domain for glutamylation[16]. It is also not clear how SidJ selectively targets E860 of SdeA, but not nearby E857 and E862 or whether it modifies proteins beyond SidEs by glutamylation or AMPylation. Glutamylation of SidEs by SidJ expands the strategies employed by *L pneumophila* to ensure balanced modulation of host function[1]. SidJ represents a unique glutamylase that bearing no similarity to mammalian glutamylases[12,21]. The requirement of CaM for its activity will ensure that SidEs will not be inactivated prior to modifying host targets[7]. CaM also activates the edema factor of *Bacillus anthracis* and CyaA of *Bordetella pertussis*[22,23], both catalyzing the synthesis of the important signaling molecule cyclic AMP[24]. Further study of the mechanism of CaM-induced activation of SidJ and the relationship between the AMPylation and glutamylation reactions will likely reveal insights into regulation and function of glutamylases.

Methods

Media, bacteria strains, plasmid constructions and cell lines

L. pneumophila strains used in this study were derivatives of the Philadelphia 1 strain Lp02[25] and were grown and maintained on CYE plates or in ACES buffered yeast extract (AYE) broth as previously described[25]. The *sidJ* in-frame deletion strain had been decribed[5]. *sidJ* and *sdeA* genes and their mutants were cloned into pZLQ[26] or pZL507[27] for complementation. The *E. coli* strains XL1-Blue and BL21(DE3) were used for expression

Author Manuscript Author Manuscript Author Manuscript Author Manuscript

and purification of all the recombinant proteins used in this study. *E. coli* strains were grown in LB. Genes for protein purifications were cloned into pQE30 (QIAGEN), pGEX-6P-1 (Amersham) and pET-21a (Novagen) for expression. For ectopic expression of proteins in mammalian cells, genes were inserted into the 4xFlag CMV vector[2] or the 3xHAcDNA3.1 vector[28]. HEK293T cells was cultured in Dulbecco's modified minimal Eagle's medium (DMEM) supplemented with 10% Fetal Bovine Serum (FBS). U937 cells were cultured in Roswell Park Memorial Institute 1640 (RPMI 1640) medium supplemented with 10% FBS. The yeast strains BY4741 and W303 were used for toxicity assays. Yeast strains were cultured in YPD media containing yeast extract, peptone and glucose, or SD minimal media containing yeast nitrogen base, glucose and amino acid drop-out mix for selection of transformed plasmids. For GAL1 promoter induction, 2% galactose was used to replace 2% glucose as the sole carbon source in minimal media. To examine the yeast toxicity of SidJ and its mutants, each allele was cloned into pYES1NTA (Invitrogen) which contains GAL1 promoter for inducible expression in yeast[14]. *cmd1* gene was cloned into p415ADH[29] for expression in yeast. For the suppression of SdeA yeast toxicity by SidJ, *sdeA* and its mutants were expressed from pYES1NTA and SidJ was expressed from p425GPD[29]. All mammalian cell lines were regularly checked for potential mycoplasma contamination by the universal mycoplasma detection kit from ATCC (cat# 30–1012K).

Transfection, infection, immunoprecipitation

Lipofectamine 3000 (Thermo Fisher Scientific) was used to transfect HEK293T cells grown to about 70% confluence. Different plasmids were transfected into HEK293T cells respectively. Transfected cells were collected and lysed with the Radioimmunoprecipitation assay buffer (RIPA buffer, Thermo Fisher Scientific) at 16–18 h post transfection. Or infected with indicated bacterial strains. When needed, immunoprecipitation was performed with lysates of transfected cells with HA-specific antibody coated agarose beads (Sigma cat#A2095), Flag-specific antibody coated agarose beads (Sigma cat#F1804), or CaM-coated agarose beads (Sigma cat#A6112) at 4°C for 4 h. Beads were washed with pre-cold RIPA buffer or respective reaction buffers for 3 times. Samples were resolved by SDS-PAGE gels and followed by immunoblotting analysis with the specific antibodies, or silver staining following the manufacturer's protocols (Sigma cat#PROTSIL1).

For infection experiments, *L. pneumophila* strains were grown to the post-exponential phase (OD_{600}=3.3–3.8) in AYE broth. When necessary, complementation strains were induced with 0.2 mM IPTG for 3 h at 37°C before infection. U937 cells were infected with *L. pneumophila* strains correspondingly. Cells were collected and lysed with 0.2% saponin on ice for 30 min. Cell lysates were resolved by SDS-PAGE and followed by immunoblotting analysis with the specific antibodies, respectively. *L. pneumophila* bacteria lysates were resolved by SDS-PAGE followed by immunoblotting with the SidJ and SdeA specific antibodies to examine the expression of SidJ and SdeA, and isocitrate dehydrogenase (ICDH) was probed as loading controls with antibodies previously described[27].

For intracellular growth in *Acanthamoeba castellanii* cells, infection was performed at an MOI of 0.05 and the total bacterial counts were determined at 24 h intervals as described[20].

Author Manuscript Author Manuscript Author Manuscript Author Manuscript

A. castellanii was maintained in HL5 medium. For infection, HL5 medium was replaced by MB medium with 1 mM IPTG added to overexpress indicated proteins.

Protein purification

Ten mL overnight *E. coli* cultures were transferred to 400 mL LB medium supplemented with 100 μg/mL of ampicillin and the cultures were grown to OD_{600} of 0.6~0.8 prior to the induction with 0.2 mM IPTG. Cultures were further incubated at 18°C for overnight. Bacteria were collected by centrifugation at 4,000*g* for 10 min, and were lysed by sonication in 30 mL PBS. Bacteria lysates were centrifuged twice at 18,000*g* at 4°C for 30 min to remove insoluble fractions and unbroken cells. Supernatant containing recombinant proteins were incubated with 1 mL Ni^{2+}-NTA beads (Qiagen) or glutathione agarose beads (Pierce) at 4°C for 2 h with agitation. Ni^{2+}-NTA beads with bound proteins were washed with PBS buffer containing 20 mM imidazole for 3 times, 30x of the column volume each time. Proteins were eluted with PBS containing 300 mM imidazole. Glutathione agarose beads were washed with a Tris buffer (50 mM Tris-HCl (pH 8.0)) and eluted with 10 mM reduced glutathione in the same buffer. Proteins were dialyzed in buffer containing 25 mM Tris-HCl (pH 7.5), 150 mM NaCl and 1 mM dithiothreitol (DTT) for 16–18 h. The native $SidJ_{\Delta N99}$ was purified by similar protocol and the CaM proteins purification is similar with this process with 2 mM $CaCl_2$ and 10% Glycol added. For crystallization, the SidJ-CaM complex formed by mixing these two proteins in 20 mM Tris-HCl (pH 8.0), 150 mM NaCl, 2 mM $CaCl_2$.

For protein purifications from mammalian cells. HEK293T cells were transfected with corresponding plasmids to express Flag tagged proteins. Cells were lysed with the RIPA buffer, and subjected immunoprecipitation with the Flag specific antibody coated beads. Then proteins were eluted from beads by using 3xFlag peptides following the manufacturer's protocols (Sigma cat#F4799).

Crystallization

The purity of $SidJ_{\Delta N99}$-CaM was ~ 95% as assessed by SDS-PAGE and initial crystallization screens of native SidJ-CaM were conducted via sitting-drop vapor diffusion using commercial crystallization screens. The protein concentration used for crystallization was 5–7 mg/ml. Hampton Research kits were used in the sitting drop vapor diffusion method to get preliminary crystallization conditions at 16°C. Crystallization drops contained 0.5 μL of the protein solution mixed with 0.5 μL of reservoir solution. Diffraction quality crystals of $SidJ_{\Delta N99}$-CaM and its complex with ATP ($SidJ_{\Delta N99}$-CaM-ATP) were grown in the presence of 0.1 M HEPES (pH 6.5–7.5), 20% (v/v) PEG 4000, and 0.2 M NaCI. To solve the phase problem, Se-Met was incorporated into SidJ and the $SidJ_{Se\text{-}Met}$ was purified similarly to native SidJ except with inclusion of 5 mM DTT added to the buffer during all the purification process. The protein concentration of $SidJ_{Se\text{-}Met}$-CaM used for crystallization was also ~7 mg/ml. Diffraction quality crystals of $SidJ_{Se\text{-}Met}$-CaM were grown and optimized in the same condition. All crystals were flash frozen in liquid nitrogen, with addition of 20%−25% (v/v) glycerol as cryoprotectant.

Author Manuscript Author Manuscript Author Manuscript Author Manuscript

Data collection and Structure determination

X-ray diffraction for Se-Met SidJ$_{\Delta N99}$-CaM, native SidJ$_{\Delta N99}$-CaM and SidJ$_{\Delta N99}$-CaM-ATP were collected at the beamline BL-17U1 of the Shanghai Synchrotron Radiation Facility (SSRF). All data were indexed and scaled using HKL2000 software[30]. The initial phase of SidJ$_{\Delta N99}$-CaM was determined by using the single-wavelength anomalous dispersion (SAD) phasing method. Phases were calculated using AutoSol implemented in PHENIX[31]. AutoBuild in PHENIX was used to automatically build the atom model. Molecular Replacement was then performed with this model as a template to determine the structure of other complexes. After several rounds of positional and B-factor refinement using Phenix. Refine with TLS parameters alternated with manual model revision using Coot[32], the quality of final models were checked using the PROCHECK program (https://www.ebi.ac.uk/thornton-srv/software/PROCHECK). The quality of the final model was validated with MolProbity[33]. Structures were analyzed with PDBePISA (Protein Interfaces, Surfaces, and Assemblies)[34], Dali (http://ekhidna2.biocenter.helsinki.fi/dali), and Details of the data collection and refinement statistics are given in Extended data Table 1. All of the figures showing structures were prepared with PyMOL (http://www.pymol.org). In the final models, the one for the SidJ$_{\Delta N99\text{-}Se\text{-}Met}$-CaM complex contained 91.05%, 8.58%, and 0.16% in the favoured, allowed and outlier regions of the Ramachandran plot, respectively. The one for the SidJ$_{\Delta N99}$-CaM complex contained 93.25%, 6.63%, and 0.10% in the favoured, allowed and outlier regions of the Ramachandran plot, respectively. The final model for the SidJ$_{\Delta N99}$-CaM-AMP complex contained 92.10%, 7.76% and 0.00% in the favoured, allowed and outliers regions, respectively of the Ramachandran plot.

Analytic Ultracentrifugation (AUC)

Sedimentation velocity experiments were used to assess the molecular sizes of the SidJ$_{\Delta N99}$-CaM complex at 20°C on a Beckman XL-A analytical ultracentrifuge equipped with absorbance optics and an An60 Ti rotor (Beckman Coulter, Inc; Fullerton, CA). Samples were diluted to an optical density at 280nm (OD_{280}) of 1 in a 1.2-cm path length. The rotor speed was set to 30,000 rpm for all samples. The sedimentation coefficient was obtained using the c(s) method with the Sedfit Software.

In vitro ubiquitination assays

For SdeA-mediated ubiquitination reaction, 0.1 μg His$_6$-SdeA, 1 μg GST-SidJ were preincubated in a 25 μL reaction system containing 50 mM Tris-HCl (pH 7.5) and 1 mM DTT, 1 mM β-NAD^+ for 2 h at 37°C. When needed, 5 mM $MgCl_2$, 1 mM L-glutamate, 1 mM ATP and 1 μM CaM (Sigma cat# C4874) were supplemented. After 2 h preincubation, a cocktail containing 1 mM β-NAD^+, 0.25 μg 4xFlag-Rab33b, 5 μg ubiquitin were supplemented into reactions and the reaction was allowed to proceed for another 2 h at 37°C.

In vitro glutamylation assays

0.1 μg His$_6$-SdeA, 1 μg GST-SidJ were incubated in a 25 μL reaction system containing 50 mM Tris-HCl (pH 7.5) and 1 mM DTT, 5 mM $MgCl_2$, 1 mM L-glutamate. 1 mM ATP and 1 μM CaM for 2 h at 37°C. To measure the glutamylase activity of SidJ using ^{14}C-glutamate, 2 μg His$_6$-SdeA and 0.5 μg GST-SidJ were incubated in a 25 μL reaction system containing

Author Manuscript Author Manuscript Author Manuscript Author Manuscript

50 mM Tris-HCl (pH 7.5), 1 mM DTT, 5 mM $MgCl_2$, 1 μCi ^{14}C-L-glutamate (Perkin Elmer cat# NEC290E050UC), 1 mM ATP and 1 μM CaM for 2 h at 37°C. Products were resolved by SDS-PAGE gel and stained with Coomassie brilliant blue. Gels were then dried and signals were detected with x-ray films with a BioMax TranScreen LE (Kodak) for 3 d in −80°C.

In vitro AMPylation assays

Two μg GST-SidJ was incubated in a 25 μL reaction system containing 50 mM Tris-HCl (pH 7.5), 1 μM CaM, 1 mM DTT, 5 mM $MgCl_2$ and 5 μCi ATP-α-^{32}P (Perkin Elmer cat# BLU003H250UC) for 2 h at 37°C. When needed 3 μg His_6-SdeA, 1 mM L-Glu were supplemented. Products were resolved by SDS-PAGE gel and stained with Coomassie brilliant blue. Gels were then dried and signals were detected with x-ray films.

HPLC analysis of glutamylation reactions

Fourty μg $SidJ_{\Delta N99}$ was incubated with 1 mM ATP in a 100 μL reaction system containing 50 mM Tris-HCl (pH 7.5) 50 mM NaCl for 4 h at 37°C. When needed 1 mM CaM, 2 mM L-Glu, 80 μg SdeA or $SdeA_{E860A}$ were supplemented. Samples were injected into a Waters Acquity UPLC equipped with a C18 reversed-phase column and a UV detector. Components were eluted isocratically with 100% H_2O for 2 minutes followed by a 10-minute gradient to 95% H_2O and 5% acetonitrile. 1 mM ATP and AMP were run as standards.

Antibodies and Immunoblotting

Purified His_6-GFP was used to raise rabbit specific antibodies using a standard protocol (Pocono Rabbit Farm & Laboratory). The antibodies were affinity purified as describe[20]. Antibodies specific for SidJ and SdeA had been described[2,5]. Commercial antibodies used are listed as below: anti-Flag (Sigma, Cat# F1804), 1: 2000; anti-HA (Roche, cat# 11867423001 1:5,000), anti-ICDH[27], 1:10,000, anti-tubulin (DSHB, E7) 1:10,000, anti-HIF-1α (R&D systems, cat#MAB1536 1:1,000), anti-PGK1 (Abcam, cat# ab113687 1:2,500), anti-CaM (Millipore, cat#05–173 1:2,000). Membranes were then incubated with an appropriate IRDye infrared secondary antibody and scanned using an Odyssey infrared imaging system (Li-Cor's Biosciences).

Constitution of the SidJ-CaM complex and size exclusion chromatography

Proteins purified as described above were further purified using a size exclusion chromatography column (Superdex 200 increase 10/300; GE Healthcare) equilibrated with a washing buffer (20 mM Tris-HCl pH 8.0,150 mM NaCl) on an AKTA pure system (GE Healthcare). To constitute the protein complex, purified SidJ and CaM were mixed at a 1:1.2 molar ratio at 4°C for 1 h on a rotatory shaker, and the complex was purified by size exclusion chromatography using the above column. In each case, the proteins were eluted with the washing buffer. Fractions containing the protein of interest were pooled and used for further analysis.

Author Manuscript Author Manuscript Author Manuscript Author Manuscript

Liquid chromatography-tandem mass spectrometry analysis

Flag-mART domain was purified from HEK293T cells coexpressing GFP-SidJ, or GFP. After separation by SDS-PAGE, gel slices containing the protein detected by silver staining were digested as described previously[35]. The digested peptides were analyzed in C18 reversed phase column connected to a UPLC (ACQUITY, Waters) coupled to an Orbitrap mass spectrometer (Q-Exactive Plus, Thermo Fisher Scientific), using the same conditions as described previously[36]. Tandem mass spectra were converted to peak lists using DeconMSn[37] and submitted blind modification search using MODa[38] against the *L. pneumophila* sequences from GenBank. Post-translational modification candidates were confirmed by manual inspection, looking for consistent mass shifts in *b* and *y* fragment series, and by reprocessing the data with MaxQuant[39] considering the specific modifications.

Microscale Thermophoresis

The interaction between SidJ and CaM and the ATP binding activity of SidJ were measured by Microscale thermophoresis using the NanoTemper Monolith NT.115 instrument set at 20% LED and 20–40% IR-laser power. Laser on and off times were set at 30 and 5 s, respectively. Each measurement consists of 16 reaction mixtures where fluorescent-labeled SidJ concentration was set constant at 150 nM and two-fold diluted CaM ranging from 20 μM to 0.61 nM was used. For ATP binding, the concentrations of ATP used were from 100 μM to 3.05 nM, respectively. The NanoTemper Analysis 2.2.4 software was used to fit the data and to determine the K_d.

Data availability

The atomic coordinates and structure factors of the $SidJ_{Se\text{-}Met}$-CaM, SidJ-CaM and SidJ-CaM-AMP have been deposited in the Protein Data Bank (PDB) under the accession codes 6K4L, 6K4K and 6K4R, respectively.

Extended Data

Author Manuscript Author Manuscript Author Manuscript Author Manuscript

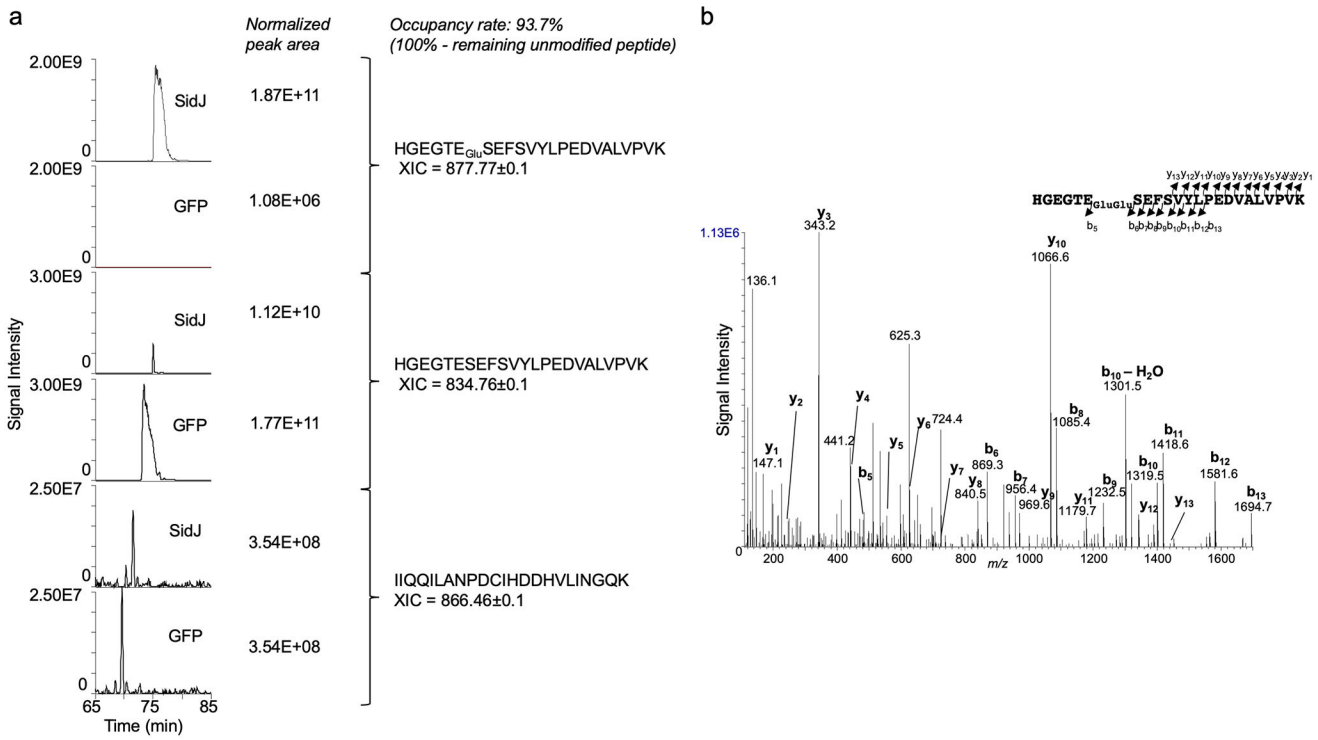

Extended Data Fig. 1. Determination of the modification rate on E860 of SdeA.

a. Peak areas of the extracted-ion chromatograms (XIC) were normalized based on the area of the unmodified peptide -I_{608}IQQILANPDCIHDDHVLINGQK$_{630-}$. The occupancy rate of glutamylation on residue was calculated based on the consumption of the unmodified -H_{855}GEGTESEFSVYLPEDVALVPVK$_{877-}$ in samples from cells cotransfected to express GFP-SidJ compared to those of controls from cells transfected to express GFP.

b. SidJ induces a 258.09 Dalton post-translation modification on E860 within the mART motif of SdeA. 4xFlag-mART purified from HEK293T cells coexpressing SidJ detected by silver staining (Fig. 2d) was analyzed by mass spectrometric analysis. Tandem mass (MS/MS) spectrum shows the fragmentation profile of the modified peptide -H_{855}GEGTE$_{GluGlu}$SEFSVYLPEDVALVPVK$_{877-}$, including ions b_5 and b_6 that confirms the modification site at the E860 residue. In each case, similar results were obtained in three independent experiments.

Author Manuscript Author Manuscript Author Manuscript Author Manuscript

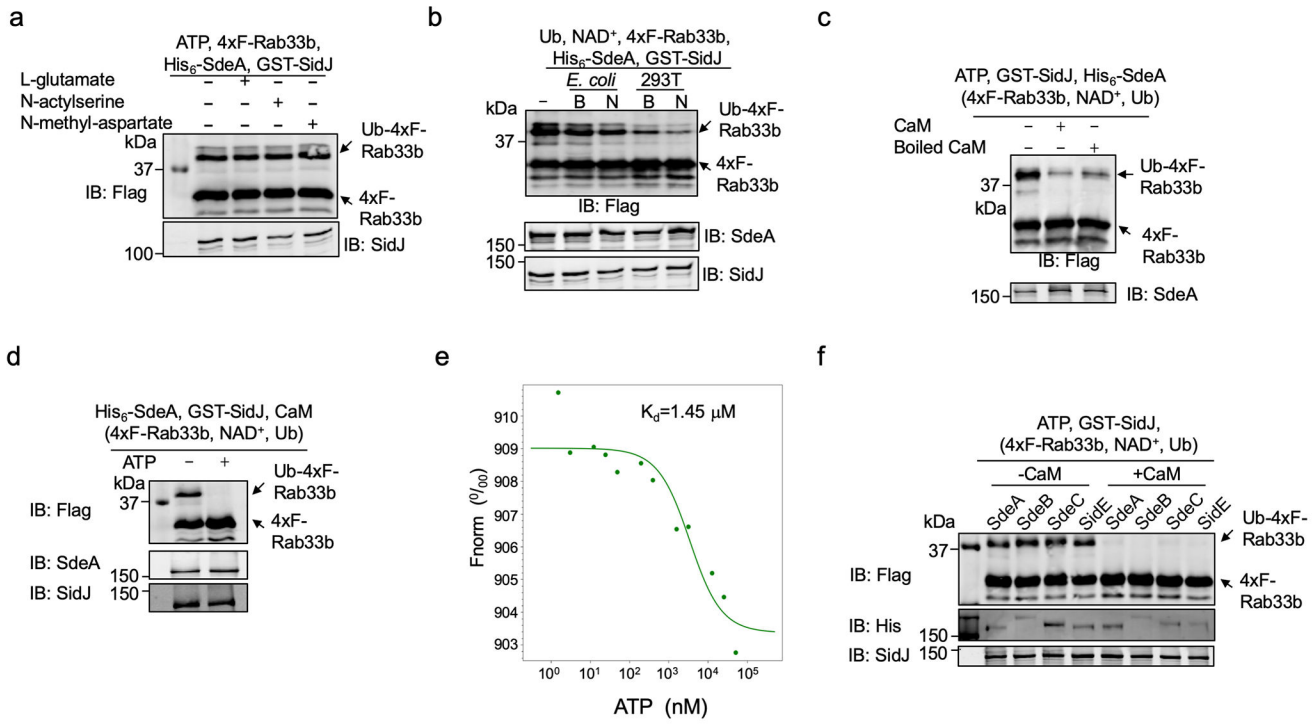

Extended Data Fig. 2. The effects of cell lysates, ATP, heat treatment on CaM on the activity of SidJ and its inhibition of the activity of all members of the SidE family.

a. Inhibition of SdeA activity does not occur in *in vitro* reactions containing L-glutamate or each of its two structural isomers. L-glutamate, N-acetylserine or N-methyl-aspartate was incubated with SdeA, SidJ and ATP for 2 h before assaying for the activity of SdeA.

b. A molecule(s) from mammalian cells is required for SidJ to inhibit SdeA. Lysates from *E. coli* or HEK293T cells were added to reactions containing SdeA and SidJ for 2 h before measuring the activity of SdeA.

c. Heat treatment does not completely abolish CaM activity. CaM or CaM treated by heating at 100°C for 5 min was included in reactions that allow glutamylation of SdeA for 2 h. A cocktail containing 4xF-Rab33b, NAD^+ and ubiquitin was added to each reaction. Samples were resolved by SDS-PAGE and detected for Rab33b ubiquitination after another 2 h incubation at 37°C.

d. The activity of SidJ requires ATP. His_6-SdeA was incubated with GST-SidJ, L-glutamate and CaM in reactions with or without 1 mM ATP for 2 h, 4xF-Rab33b, NAD^+ and ubiquitin were added to each reaction. After another 2 h incubation, the activity of SdeA was evaluated by the production of ubiquitinated Ra33b. Protein components in the reactions were detected by immunoblotting with specific antibodies.

e. The binding of ATP by SidJ. Binding of ATP by purified SidJ was evaluated using Microscale thermophoresis in which the concentration of SidJ was kept constant. The dissociation constant (K_d) was determined by the NanoTemper Analysis 2.2.4 software.

f. SidJ inhibits the activity of members of the SidE family. Recombinant protein of each of SidE family protein was incubated with ATP, L-glutamate and GST-SidJ in the presence or absence of CaM for 2 h, a cocktail containing 4xF-Rab33b, NAD^+ and ubiquitin was added to the reactions. After additional 2 h incubation, modification of Rab33b was detected by

Author Manuscript Author Manuscript Author Manuscript Author Manuscript

immunoblotting with a Flag-specific antibody. The formation of Ub-4xF-Rab33b is indicated by a shift in molecular weight. In each panel, data shown were one representative from at least three independent experiments that had similar results.

Author Manuscript Author Manuscript Author Manuscript Author Manuscript

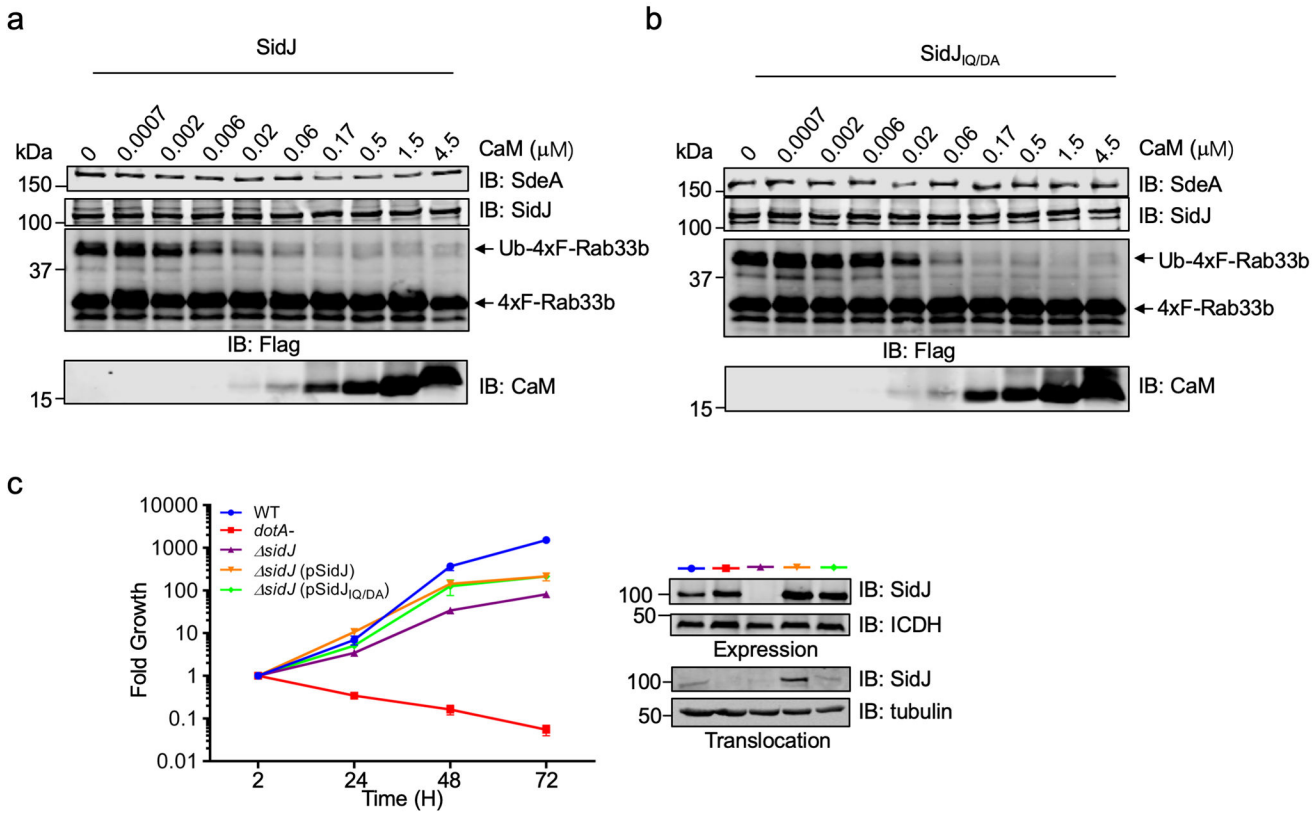

Extended Data Fig. 3. The IQ motif of SidJ is required for its optimal response to CaM

a-b. The IQ motif is required for the optimal activity of SidJ in response to CaM. Serially diluted CaM were preincubated with SidJ (**a**) or the $SidJ_{IQ}$ mutant (**b**) and SdeA in the glutamylation buffer at 37°C for 2 h. A cocktail containing 4xFlag-Rab33b, NAD^+, and ubiquitin was added to the reactions. After incubation for another 2 h at 37°C. Proteins separated by SDS-PAGE were probed with the indicated antibodies. $SidJ_{IQ/DA,}$ I841, Q842 were mutated to Asp and Ala, respectively. In each panel, data shown were one representative from at least three independent experiments that had similar results.

c. The $SidJ_{IQ}$ mutant complements the intracellular growth defect of the *ΔsidJ* mutant. *Acanthamoeba castellanii* was infected with the indicated bacterial strains and intracellular bacteria were determined at the indicated time points. Each strain was done in triplicate and similar results were obtained in two independent experiments. Results are from one representative experiment done in triplicate from three independent experiments; error bars represent s.e.m. (n = 3).

Author Manuscript Author Manuscript Author Manuscript Author Manuscript

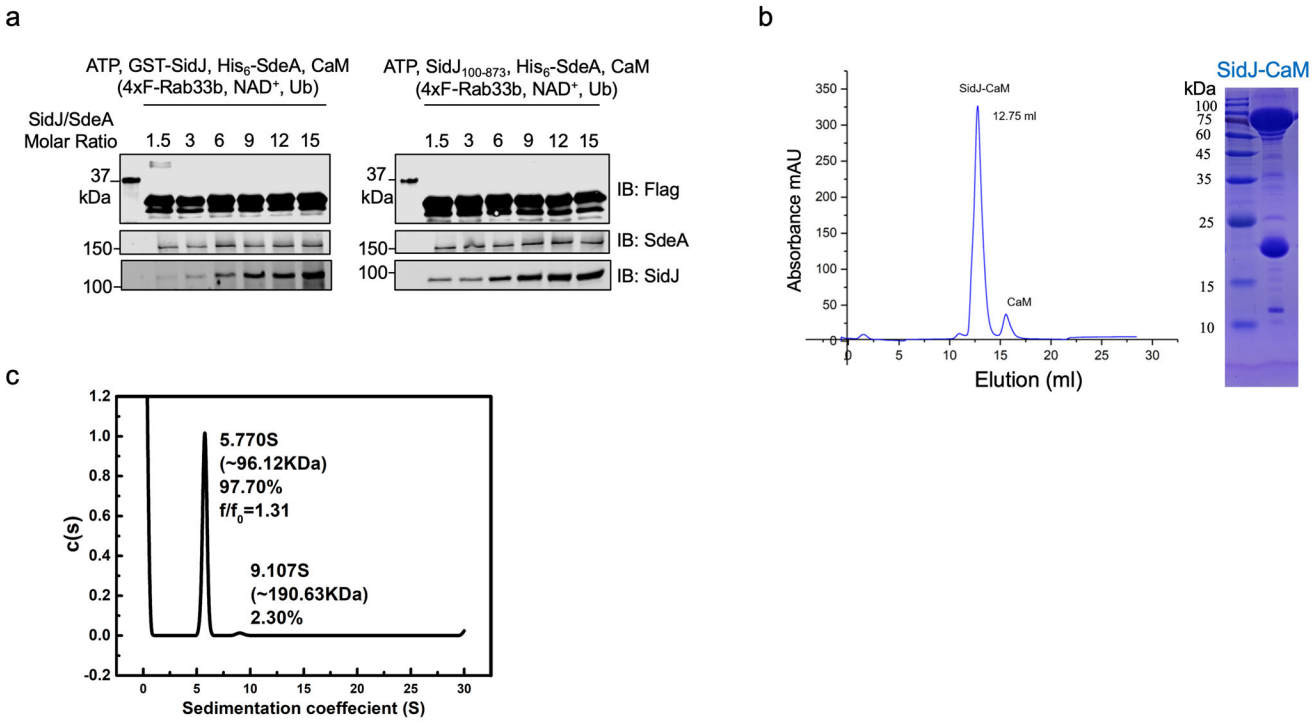

Extended Data Fig. 4. SidJ forms stable heterodimer with CaM at the molar ratio of 1:1

a. $SidJ_{\Delta N99}$ maintains the ability to inhibit SdeA activity at levels comparable to full-length SidJ. SdeA was incubated with GST-SidJ or $SidJ_{\Delta N99}$ at indicated molar ratios in reactions containing ATP, L-Glu, CaM for 2 h at 37°C. A cocktail containing 4xFlag-Rab33b, NAD^+, and ubiquitin was added to each reaction for additional 2 h at 37°C, proteins resolved by SDS-PAGE were probed with the indicated antibodies. SdeA activity was measured by the production of ubiquitinated Rab33b as indicated by a shift in molecular weight.

b. Size exclusion chromatography profiles of SidJ-CaM. Purified proteins were separated by a Superdex 200 increase 10/300 column (GE Healthcare) on an AKTA pure system (left). Fractions with strong absorbance at OD_{260} were collected and analyzed by SDS-PAGE followed by detection with Coomassie brilliant blue staining (right).

c. The heterodimer formed between $SidJ_{\Delta N99}$ with CaM is a monomer. Analytical ultracentrifugation analysis yielded a sedimentation coefficient of 5.770 S, and a molecular mass of approximately 96.12 kDa, indicating the heterodimer of $SidJ_{\Delta N99}$ and CaM. In each panel, data shown were one representative from at least three independent experiments that had similar results.

Author Manuscript Author Manuscript Author Manuscript Author Manuscript

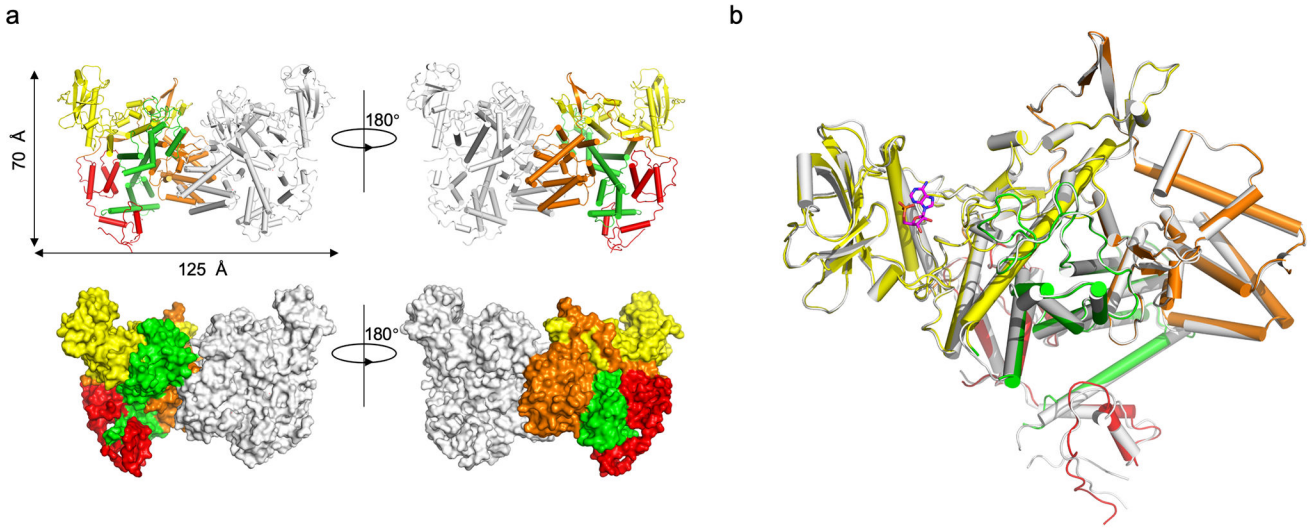

Extended Data Fig. 5. Overall structure of SidJ-CaM complex in one asymmetric unit and the comparison of complex structures with or without AMP

a. Two views of the structure of the SidJ-CaM heterodimer in the asymmetric unit (ASU) displayed as ribbon diagram (upper panel) and surface rendering (lower panel), one of the SidJ-CaM heterodimer is colored as shown in Fig. 4 and the other one is colored in grey.

b. Superimposition of the structures of the SidJ-CaM and SidJ-CaM-AMP. The SidJ-CaM-AMP ternary complex is colored as shown in Fig. 4d and SidJ-CaM binary complex is colored in grey.

Author Manuscript Author Manuscript Author Manuscript Author Manuscript

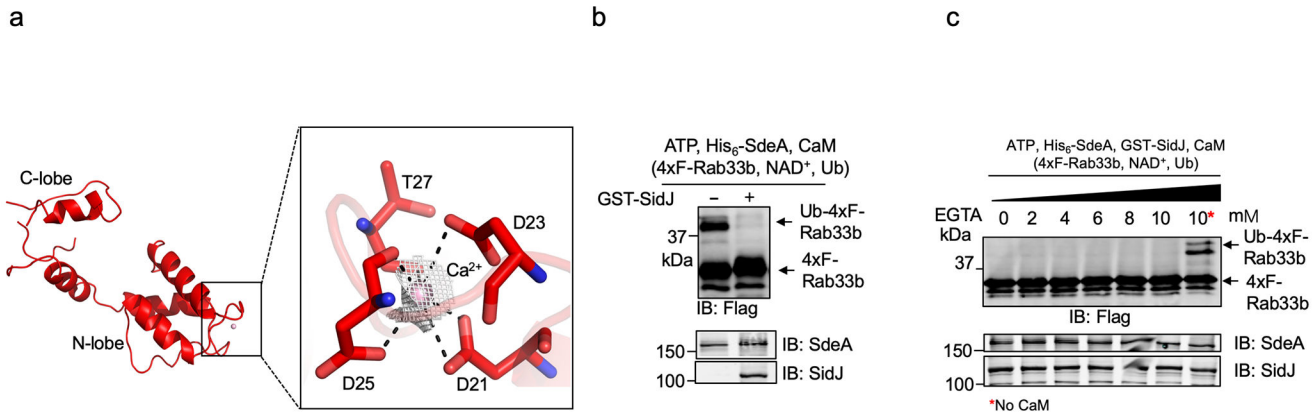

Extended Data Fig. 6. Interactions between CaM and Ca^{2+} from the crystal structures and the role of Ca^{2+} on the activation of SidJ by CaM

a. Key residues of CaM involved in the interaction with Ca^{2+}. Ca^{2+} is coordinated by D21, D23, D25 and T27 of CaM are shown in red sticks. Ca^{2+} is shown in pink sphere. Electron density of an SA Fo-Fc omit map for Ca^{2+} contoured at 3.0 σ.

b. Dialysis against 20 mM EGTA does not abolish the activity of SidJ. All proteins used in the reactions were dialyzed against a buffer containing 20 mM EGTA for 14 h. SdeA was incubated with SidJ in reactions containing ATP and dialyzed CaM for 2 h at 37°C. Reactions without SidJ were established as a control. A cocktail containing 4xFlag-Rab33b, NAD^+, and ubiquitin was added to each reaction. After further incubation for 2 h at 37°C, proteins resolved by SDS-PAGE were probed with the indicated antibodies. SdeA activity was measured by the production of ubiquitinated Rab33b as indicated by a shift in molecular weight.

c. The activity of SidJ is not sensitive to 10 mM EGTA. SdeA was first incubated with SidJ for glutamylation with indicated amounts of EGTA for 2 h at 37°C. NAD^+, 4xFlag-Rab33b and ubiquitin were then supplemented to the reactions, which were allowed to proceed for 2 h at 37°C before being resolved by SDS-PAGE. Rab33b modification was detected as described in **b**. Proteins in the reactions were detected by immunoblotting with specific antibodies. In panels **b-c**, similar results were obtained in at least three independent experiments.

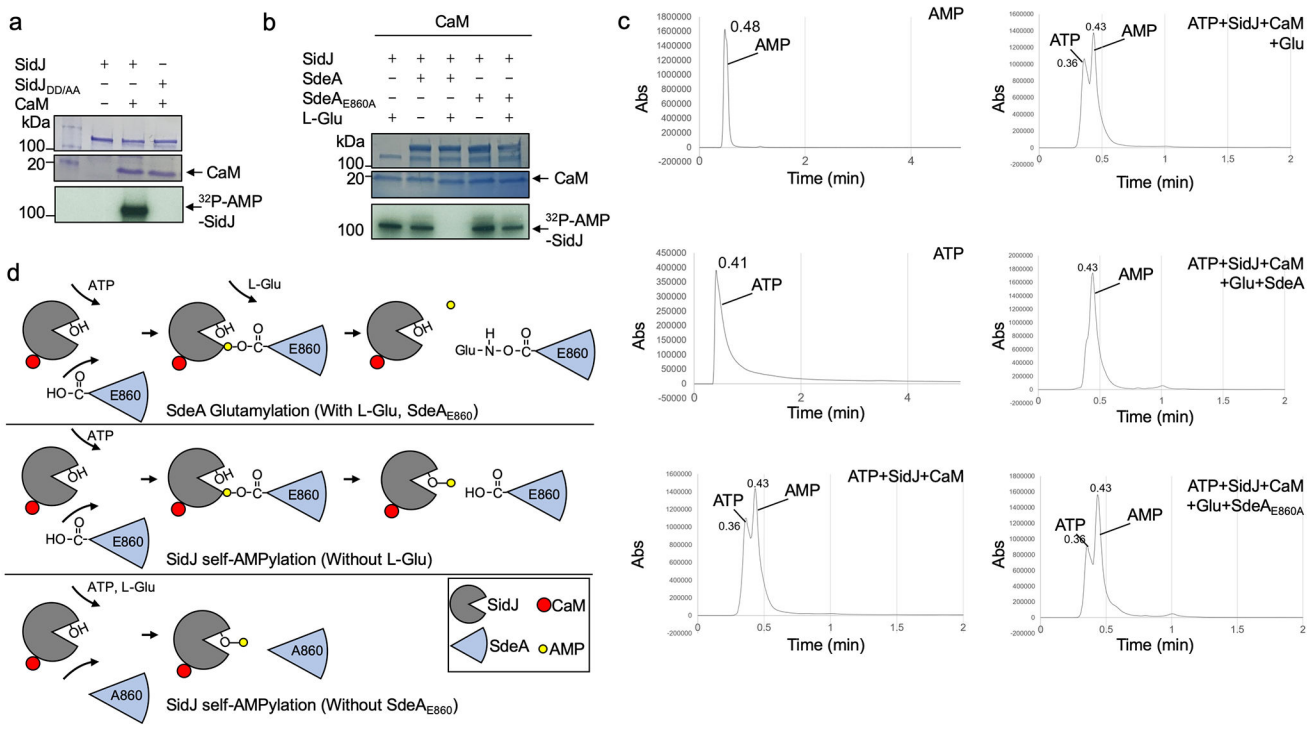

Extended Data Fig. 7. The mechanism of SidJ induced CaM dependent self-AMPlyation and SdeA glutamylation

a. SidJ induces self-AMPylation in a CaM dependent manner. SidJ was incubated with ^{32}P-α-ATP, Mg^{2+}, with or without CaM for 2 h at 37°C. After separation by SDS-PAGE, the incorporation of ^{32}P-α-ATP was detected by autoradiography.

b. SdeA glutamylation by SidJ interferes with SidJ self-AMPylation. SidJ was incubated with ^{32}P-α-ATP, Mg^{2+}, CaM for 2 h at 37°C. When needed L-Glu, SdeA, $SdeA_{E860A}$ were supplemented. After separation by SDS-PAGE, the incorporation of ^{32}P-α-ATP was detected by autoradiography.

c. SdeA glutamylation by SidJ accelerates ATP hydrolysis and AMP release. SidJ was incubated with indicated components for 2 h at 37°C. Samples were analyzed by HPLC. AMP and ATP were used as standard. In panels **a-c**, data shown were one representative from at least three independent experiments that had similar results.

d. Schematic model of SidJ induced glutamylation and AMPylation. SidJ incudes glutamylation on $SdeA_{E860}$ when ATP and L-Glu are supplemented in reaction. In reactions missing L-Glu or modifiable SdeA, SidJ induces self-AMPylation.

Author Manuscript Author Manuscript Author Manuscript Author Manuscript

Author Manuscript
Author Manuscript
Author Manuscript
Author Manuscript

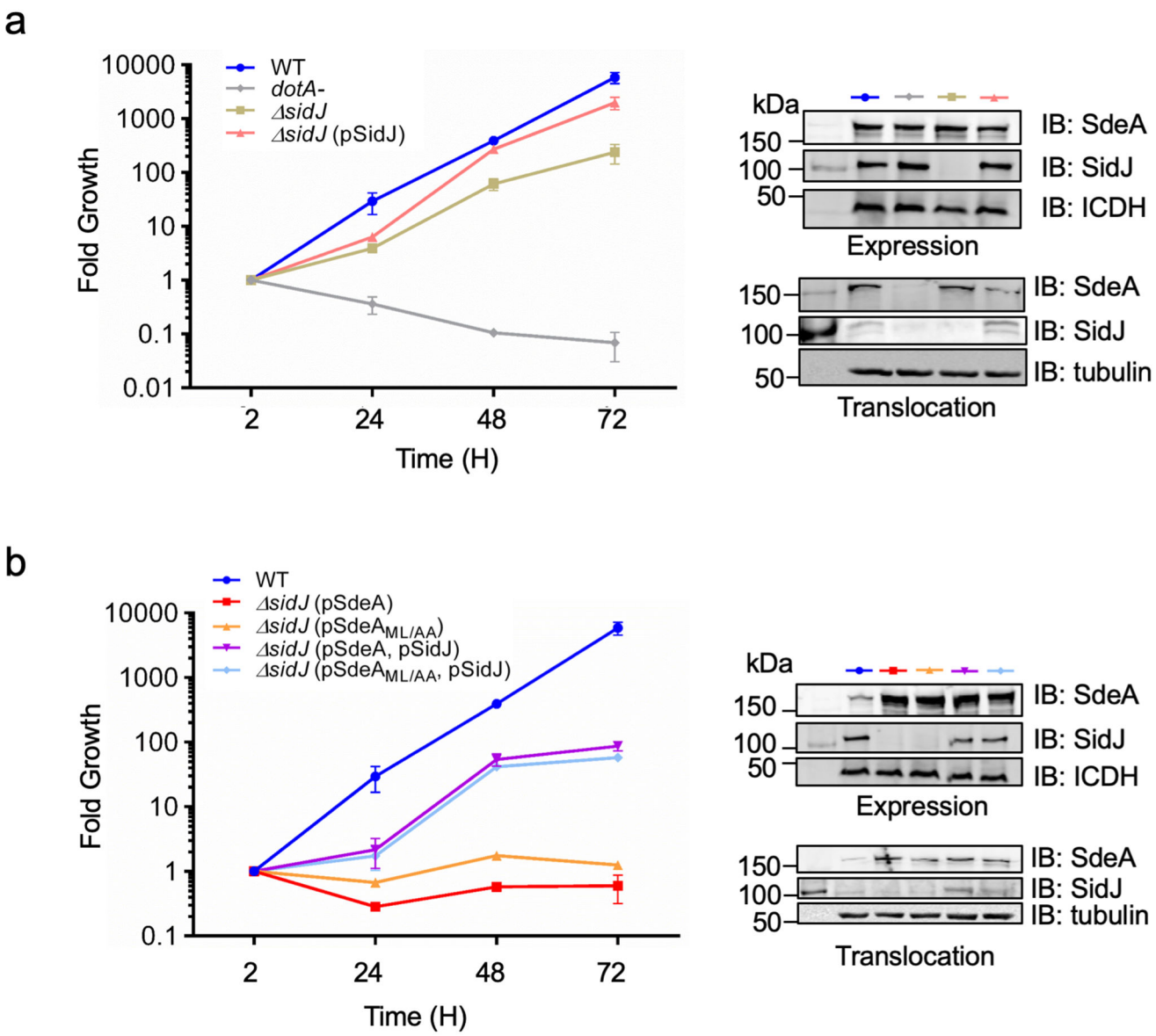

Extended Data Fig. 8. Intracellular growth phenotypes associated the *sidJ* mutant expressing SdeA and its mutants.

a. Intracellular defects of the *L. pneumophila* Δ*sidJ* mutant can be complemented by SidJ expressed from a multicopy plasmid. The indicated strains were used to infect *A. castellanii* at an MOI of 0.05 and the growth of the bacteria was evaluated at 24 h intervals. Fold growth was calculated based on total bacterial counts at the indicated time points and those of the 2 h point.

b. Overexpression of a SdeA mutant defective in substrate recognition inhibits intracellular growth of the Δ*sidJ* mutant. Intracellular growth of the indicated *L. pneumophila* strains in *A. castellanii* was evaluated as described in **a**. In each panel, the expression of SidJ, SdeA and its mutants in bacterial cells and their translocation into infected cells was determined by immunoblotting from total bacterial cell lysates and the saponin-soluble fraction of infected cells, with ICDH and tubulin as loading controls, respectively (right panels). In each

Author Manuscript Author Manuscript Author Manuscript Author Manuscript

case, results are from one representative experiment done in triplicate from three independent experiments; error bars represent s.e.m. (n = 3).

Author Manuscript Author Manuscript Author Manuscript Author Manuscript

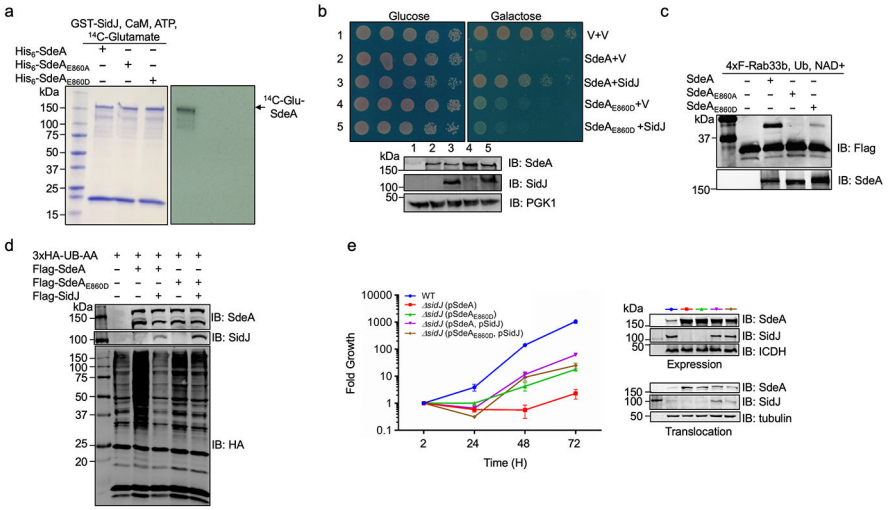

Extended data Fig. 9. SidJ functions to regulate the activity of SdeA during *L. pneumophila* infection

a. $SdeA_{E860D}$ is resistant to glutamylation catalyzed by SidJ. SdeA, $SdeA_{E860A}$ or $SdeA_{E860D}$ was added to reactions containing GST-SidJ, ^{14}C-glutamate ATP and CaM and the reactions were allowed to proceed for 2 h at 37°C. After separation by SDS-PAGE, the incorporation of ^{14}C-glutamate was detected by autoradiography.

b. Yeast toxicity induced by $SdeA_{E860D}$ cannot be suppressed by SidJ. A plasmid that directs the expression of SidJ was introduced into yeast strains expressing SdeA or $SdeA_{E860D}$ from a galactose inducible promoter, serially diluted yeast cells were spotted onto glucose or galactose medium for 2 d and the growth of the cells was evaluated by imaging (upper panels). The expression of SidJ, SdeA and $SdeA_{E860D}$ was determined by immunoblotting with specific antibodies. The PGK1 (3-phosphoglyceric phosphokinase-1) was probed as a loading control (lower panels).

c. $SdeA_{E860D}$ still ubiquitinates Rab33b. Reactions containing the indicated components were allowed to proceed for 2 h at 37°C, samples were then resolved by SDS-PAGE and ubiquitination of Rab33b was probed by immunoblotting with a Flag-specific antibody to detect the production of modified Rab33b with a higher molecular weight.

d. $SdeA_{E860D}$-mediated protein ubiquitination in mammalian cells is insensitive to SidJ. HEK293T cells were transfected to express the indicated proteins for 16-18 h. Cleared cell lysates were subjected to SDS-PAGE and immunoblotting with an HA specific antibody to detected proteins ubiquitinated by 3xHA-Ub-AA. The levels of SdeA, $SdeA_{E860D}$ and SidJ were assessed by antibodies specific for these proteins. Note that coexpression of SidJ reduced the ubiquitination induced by SdeA but not $SdeA_{E860D}$. In panels **a-d**, data shown were one representative from at least three independent experiments that had similar results.

e. The effects of SidJ on intracellular growth defect caused by overexpression of SdeA or $SdeA_{E860D}$. The indicated *L. pneumophila* strains were used to infect *Acanthamoeba castellanii* at an MOI of 0.05 and the growth of the bacteria was evaluated at 24 h intervals. Fold growth was calculated based on total bacterial counts at the indicated time points. Note that the difference between strain Δ*sidJ* (pSdeA) and Δ*sidJ* (pSdeA, pSidJ). The growth defect caused by overexpressing the $SdeA_{E860D}$ mutant cannot be rescued by SidJ. The levels of relevant proteins in bacterial cells and in infected cells were probed by

Author Manuscript Author Manuscript Author Manuscript Author Manuscript

immunoblotting from total bacterial cell lysates and the saponin-soluble fraction of infected cells, with ICDH and tubulin as loading controls, respectively (right panels). Results showen are from one representative experiment done in triplicate from three independent experiments; error bars represent s.e.m. (n = 3).

Extended Data Table 1

Data collection and refinement statistics

	$SidJ_{se\text{-}Met}$-CaM (PDB 6K4L)	**SidJ-CaM (PDB 6K4K)**	**SidJ-CaM-AMP (PDB 6K.4R)**
Data Collection			
Space group	$P\,1\,2_1\,1$	$P\,1\,2_1\,1$	$P\,1\,2_1\,1$
Cell dimensions			
a, *b*, *c* (Å)	61.06, 159.25, 135.81	60.96, 159.53, 135.61	60.85, 159.18, 135.03
α, β, γ (°)	90.00, 101.68, 90.00	90.00, 101.89, 90.00	90.00, 101.78,90.00
Wavelength (Å)	0.9792	0.9792	0.9792
Resolution (Å)	66.50-2.95 (3.01-2.95)*	55.46-2.71 (2.81-2.71)	66.09-3.11 (3.22-3.11)
R_{merge}	0.158 (0.959)	0.176 (1.401)	0.230 (1.131)
$I/\sigma I$	12.8 (2.5)	12.1 (2.2)	12.5 (2.3)
Completeness (%)	99.90 (100.00)	96.87 (97.82)	92.45 (99.80)
Redundancy	6.8 (7.1)	12.9(12.2)	6.5 (5.4)
Refinement			
Resolution (Å)	2.95	2.71	3.11
No. reflections	53475	66262	41852
R_{work}/R_{free}	0.252/0.278	0.205/0.243	0.239/0.279
No. atoms			
Protein	12936	12738	12640
Ligand/ion	2	2	100
Water	16	2	0
B factors (Å^2)			
Protein	58.30	69.39	65.00
Ligand/ion	64.10	128.39	75.65
R.m.s. deviations			
Bond lengths (Å)	0.005	0.006	0.003
Bond angles (°)	0.89	0.93	0.63

*For each structure one crystal was used. Values in parentheses are for highest-resolution shell.

Supplementary Material

Refer to Web version on PubMed Central for supplementary material.

Acknowledgements

We thank Dr. Chengpeng Fan of Wuhan University for assistance in structure determination and helpful discussion and Mr. Karl Weitz for assistance with the mass spectrometry analysis. This work was supported in part National Institutes of Health grants R01AI127465 and R01GM126296, the National Natural Science Foundation of China grants 31770948, 31570875 and 31200559 (SO) and by research fund from the First Hospital of Jilin University. Mass spectrometry analysis was performed in the Environmental Molecular Sciences Laboratory, a U.S.

Author Manuscript Author Manuscript Author Manuscript Author Manuscript

Department of Energy (DOE) national scientific user facility at Pacific Northwest National Laboratory (PNNL) in Richland, WA. Battelle operates PNNL for the DOE under contract DE-AC05–76RLO01830. The diffraction data were collected at the beamline BL-17U1 of Shanghai Synchrotron Radiation Facility (SSRF).

References

1. Qiu J & Luo ZQ Legionella and Coxiella effectors: strength in diversity and activity. Nat Rev Microbiol 15, 591–605, doi:10.1038/nrmicro.2017.67 (2017). [PubMed: 28713154]
2. Qiu J et al. Ubiquitination independent of E1 and E2 enzymes by bacterial effectors. Nature 533, 120–124, doi:10.1038/nature17657 (2016). [PubMed: 27049943]
3. Bhogaraju S et al. Phosphoribosylation of Ubiquitin Promotes Serine Ubiquitination and Impairs Conventional Ubiquitination. Cell 167, 1636–1649.e1613, doi:10.1016/j.cell.2016.11.019 (2016). [PubMed: 27912065]
4. Kotewicz KM et al. A Single Legionella Effector Catalyzes a Multistep Ubiquitination Pathway to Rearrange Tubular Endoplasmic Reticulum for Replication. Cell Host Microbe 21, 169–181, doi: 10.1016/j.chom.2016.12.007 (2017). [PubMed: 28041930]
5. Liu Y & Luo ZQ The Legionella pneumophila effector SidJ is required for efficient recruitment of endoplasmic reticulum proteins to the bacterial phagosome. Infect Immun 75, 592–603 (2007). [PubMed: 17101649]
6. Jeong KC, Sexton JA & Vogel JP Spatiotemporal regulation of a Legionella pneumophila T4SS substrate by the metaeffector SidJ. PLoS Pathog 11, e1004695, doi:10.1371/journal.ppat.1004695 (2015). [PubMed: 25774515]
7. Qiu J et al. A unique deubiquitinase that deconjugates phosphoribosyl-linked protein ubiquitination. Cell Res 27, 865–881, doi:10.1038/cr.2017.66 (2017). [PubMed: 28497808]
8. Lin YH & Machner MP Exploitation of the host cell ubiquitin machinery by microbial effector proteins. J Cell Sci 130, 1985–1996, doi:10.1242/jcs.188482 (2017). [PubMed: 28476939]
9. Song L & Luo ZQ Post-translational regulation of ubiquitin signaling. J Cell Biol 218, 1776–1786, doi:10.1083/jcb.201902074 (2019). [PubMed: 31000580]
10. Dorer MS, Kirton D, Bader JS & Isberg RR RNA interference analysis of Legionella in Drosophila cells: exploitation of early secretory apparatus dynamics. PLoS Pathog 2, e34, doi:10.1371/journal.ppat.0020034 (2006). [PubMed: 16652170]
11. Kalayil S et al. Insights into catalysis and function of phosphoribosyl-linked serine ubiquitination. Nature 557, 734–738, doi:10.1038/s41586-018-0145-8 (2018). [PubMed: 29795347]
12. Edde B et al. Posttranslational glutamylation of alpha-tubulin. Science 247, 83–85 (1990). [PubMed: 1967194]
13. Finn RD et al. The Pfam protein families database. Nucleic Acids Res 38, D211–222, doi: 10.1093/nar/gkp985 (2010). [PubMed: 19920124]
14. Heidtman M, Chen EJ, Moy MY & Isberg RR Large-scale identification of Legionella pneumophila Dot/Icm substrates that modulate host cell vesicle trafficking pathways. Cellular Microbiology 11, 230–248, doi:10.1111/j.1462-5822.2008.01249.x (2009). [PubMed: 19016775]
15. Rhoads AR & Friedberg F Sequence motifs for calmodulin recognition. FASEB J 11, 331–340, doi:10.1096/fasebj.11.5.9141499 (1997). [PubMed: 9141499]
16. Black MH et al. Bacterial pseudokinase catalyzes protein polyglutamylation to inhibit the SidE-family ubiquitin ligases. Science 364, 787–792, doi:10.1126/science.aaw7446 (2019). [PubMed: 31123136]
17. Van Petegem F, Chatelain FC & Minor DL Jr. Insights into voltage-gated calcium channel regulation from the structure of the CaV1.2 IQ domain-Ca2+/calmodulin complex. Nat Struct Mol Biol 12, 1108–1115, doi:10.1038/nsmb1027 (2005). [PubMed: 16299511]
18. Bagshaw C ATP analogues at a glance. J Cell Sci 114, 459–460 (2001). [PubMed: 11171313]
19. Casey AK & Orth K Enzymes Involved in AMPylation and deAMPylation. Chem Rev 118, 1199–1215, doi:10.1021/acs.chemrev.7b00145 (2018). [PubMed: 28819965]
20. Luo ZQ & Isberg RR Multiple substrates of the Legionella pneumophila Dot/Icm system identified by interbacterial protein transfer. Proc Natl Acad Sci U S A 101, 841–846 (2004). [PubMed: 14715899]

Author Manuscript Author Manuscript Author Manuscript Author Manuscript

21. O'Hagan R et al. Glutamylation Regulates Transport, Specializes Function, and Sculpts the Structure of Cilia. Curr Biol 27, 3430–3441 e3436, doi:10.1016/j.cub.2017.09.066 (2017). [PubMed: 29129530]
22. Drum CL et al. Structural basis for the activation of anthrax adenylyl cyclase exotoxin by calmodulin. Nature 415, 396–402, doi:10.1038/415396a (2002). [PubMed: 11807546]
23. Guo Q et al. Structural basis for the interaction of Bordetella pertussis adenylyl cyclase toxin with calmodulin. EMBO J 24, 3190–3201, doi:10.1038/sj.emboj.7600800 (2005). [PubMed: 16138079]
24. Gancedo JM Biological roles of cAMP: variations on a theme in the different kingdoms of life. Biol Rev Camb Philos Soc 88, 645–668, doi:10.1111/brv.12020 (2013). [PubMed: 23356492]
25. Berger KH & Isberg RR Two distinct defects in intracellular growth complemented by a single genetic locus in Legionella pneumophila. Mol Microbiol 7, 7–19 (1993). [PubMed: 8382332]
26. Luo ZQ & Farrand SK Signal-dependent DNA binding and functional domains of the quorum-sensing activator TraR as identified by repressor activity. Proceedings of the National Academy of Sciences of the United States of America 96, 9009–9014, doi:DOI 10.1073/pnas.96.16.9009 (1999). [PubMed: 10430886]
27. Xu L et al. Inhibition of host vacuolar H+-ATPase activity by a Legionella pneumophila effector. PLoS Pathog 6, e1000822, doi:10.1371/journal.ppat.1000822 (2010). [PubMed: 20333253]
28. Sheedlo MJ et al. Structural basis of substrate recognition by a bacterial deubiquitinase important for dynamics of phagosome ubiquitination. Proc Natl Acad Sci U S A 112, 15090–15095, doi: 10.1073/pnas.1514568112 (2015). [PubMed: 26598703]
29. Mumberg D, Muller R & Funk M Yeast Vectors for the Controlled Expression of Heterologous Proteins in Different Genetic Backgrounds. Gene 156, 119–122, doi:Doi 10.1016/0378-1119(95)00037-7 (1995). [PubMed: 7737504]
30. Otwinowski Z & Minor W [20] Processing of X-ray diffraction data collected in oscillation mode. Methods Enzymol 276, 307–326, doi:10.1016/s0076-6879(97)76066-x (1997).
31. Adams PD et al. PHENIX: a comprehensive Python-based system for macromolecular structure solution. Acta Crystallogr D Biol Crystallogr 66, 213–221, doi:10.1107/s0907444909052925 (2010). [PubMed: 20124702]
32. Emsley P & Cowtan K Coot: model-building tools for molecular graphics. Acta Crystallogr D Biol Crystallogr 60, 2126–2132, doi:10.1107/s0907444904019158 (2004). [PubMed: 15572765]
33. Chen VB et al. MolProbity: all-atom structure validation for macromolecular crystallography. Acta Crystallogr D Biol Crystallogr 66, 12–21, doi:10.1107/s0907444909042073 (2010). [PubMed: 20057044]
34. Krissinel E & Henrick K Inference of macromolecular assemblies from crystalline state. J Mol Biol 372, 774–797, doi:10.1016/j.jmb.2007.05.022 (2007). [PubMed: 17681537]
35. Shevchenko A, Tomas H, Havlis J, Olsen JV & Mann M In-gel digestion for mass spectrometric characterization of proteins and proteomes. Nat Protoc 1, 2856–2860, doi:10.1038/nprot.2006.468 (2006). [PubMed: 17406544]
36. Gan N, Nakayasu ES, Hollenbeck PJ & Luo ZQ Legionella pneumophila inhibits immune signalling via MavC-mediated transglutaminase-induced ubiquitination of UBE2N. Nat Microbiol 4, 134–143, doi:10.1038/s41564-018-0282-8 (2019). [PubMed: 30420781]
37. Mayampurath AM et al. DeconMSn: a software tool for accurate parent ion monoisotopic mass determination for tandem mass spectra. Bioinformatics 24, 1021–1023, doi:10.1093/bioinformatics/btn063 (2008). [PubMed: 18304935]
38. Na S, Bandeira N & Paek E Fast multi-blind modification search through tandem mass spectrometry. Mol Cell Proteomics 11 (2012).
39. Tyanova S, Temu T & Cox J The MaxQuant computational platform for mass spectrometry-based shotgun proteomics. Nat Protoc 11, 2301–2319, doi:10.1038/nprot.2016.136 (2016). [PubMed: 27809316]

Author Manuscript Author Manuscript Author Manuscript Author Manuscript

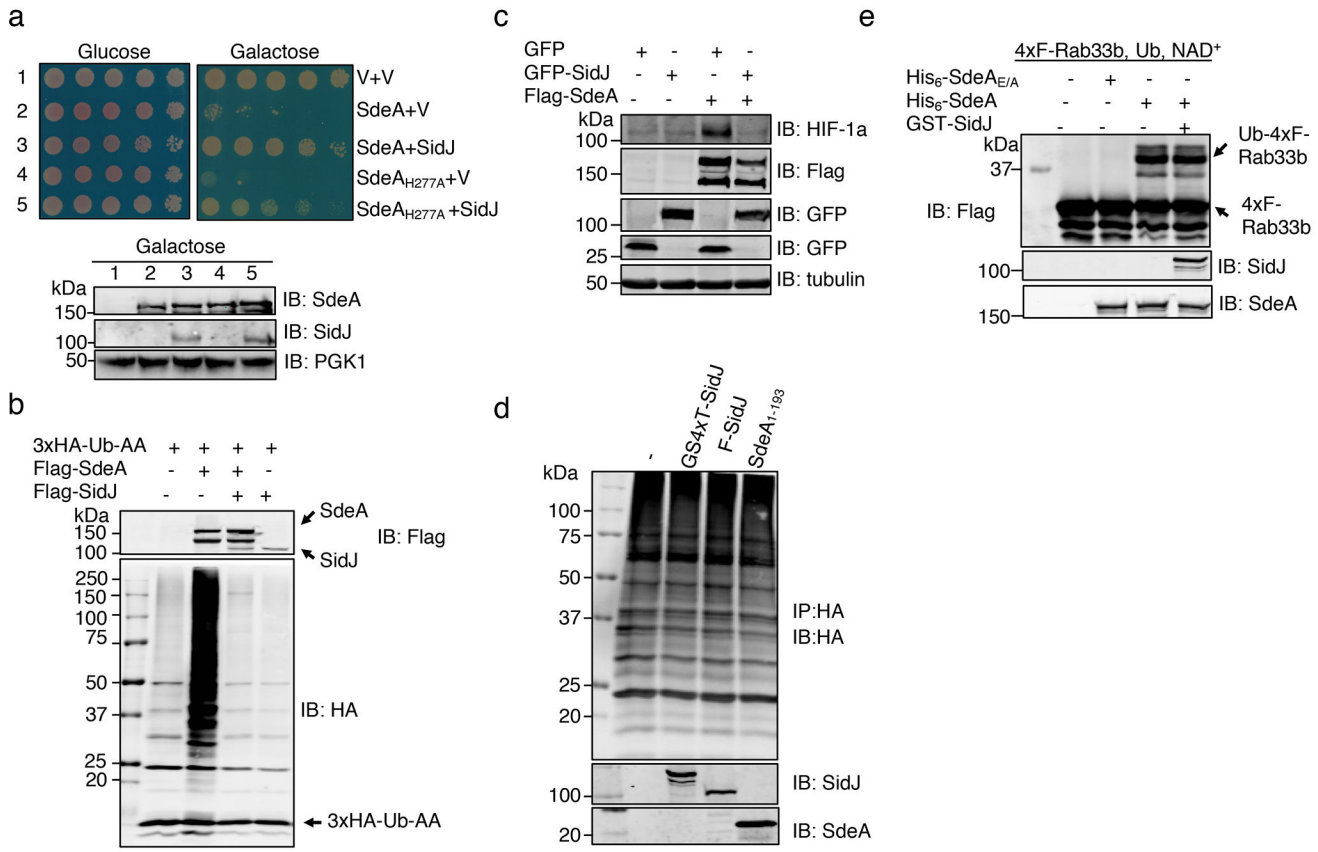

Fig. 1. SidJ antagonizes the effects of SdeA in eukaryotic cells

a. SidJ suppresses the yeast toxicity of SdeA$_{H277A}$. Diluted cells from yeast strains inducible expressing SdeA or SdeA$_{H277A}$ that harbor the vector or a SidJ construct were spotted onto the indicated media and grew for 2 d (top). The expression of relevant proteins was probed by immunoblotting (bottom). The 3-phosphoglyceric phosphokinase-1 (PGK1) was probed as a loading control. V, vector.

b. SidJ abrogates SdeA-mediated ubiquitination in mammalian cells. Lysates of HEK293T cells expressing the indicated proteins were detected by immunoblotting with an HA-specific antibody to detect 3xHA-Ub-AA and proteins modified by 3xHA-Ub-AA. The expression of Flag-SdeA and Flag-SidJ was also probed.

c. SidJ rescues HIF-1α degradation blocked by SdeA. Lysates of HEK293T cells expressing the indicated proteins were resolved by SDS-PAGE and probed with antibodies specific for the epitope tags or relevant proteins.

d. SidJ from *E. coli* or HEK293T cells cannot deubiquitinate proteins modified by SdeA. Proteins modified by 3xHA-Ub-AA obtained by immunoprecipitation were treated with GST-SidJ from *E. coli*, Flag-SidJ from HEK293T or SdeA$_{1-193}$. Note that none of these proteins caused a reduction in the ubiquitination signals.

e. GST-SidJ does not inhibit SdeA-induced ubiquitination *in vitro*. SidJ was co-incubated with SdeA for 2 h at 37°C and SdeA activity was assayed. A Flag-specific antibody was used to detect modified and unmodified 4xFlag-Rab33b, judging by a shift in its molecular weight. SdeA and SidJ were probed with specific antibodies. SdeA$_{E/A}$ is a SdeA mutant

defective in the mART activity carrying E860A and E862A mutations. The experiment in each panel was performed independently for at least 3 times with similar results.

Author Manuscript Author Manuscript Author Manuscript Author Manuscript

Author Manuscript Author Manuscript Author Manuscript Author Manuscript

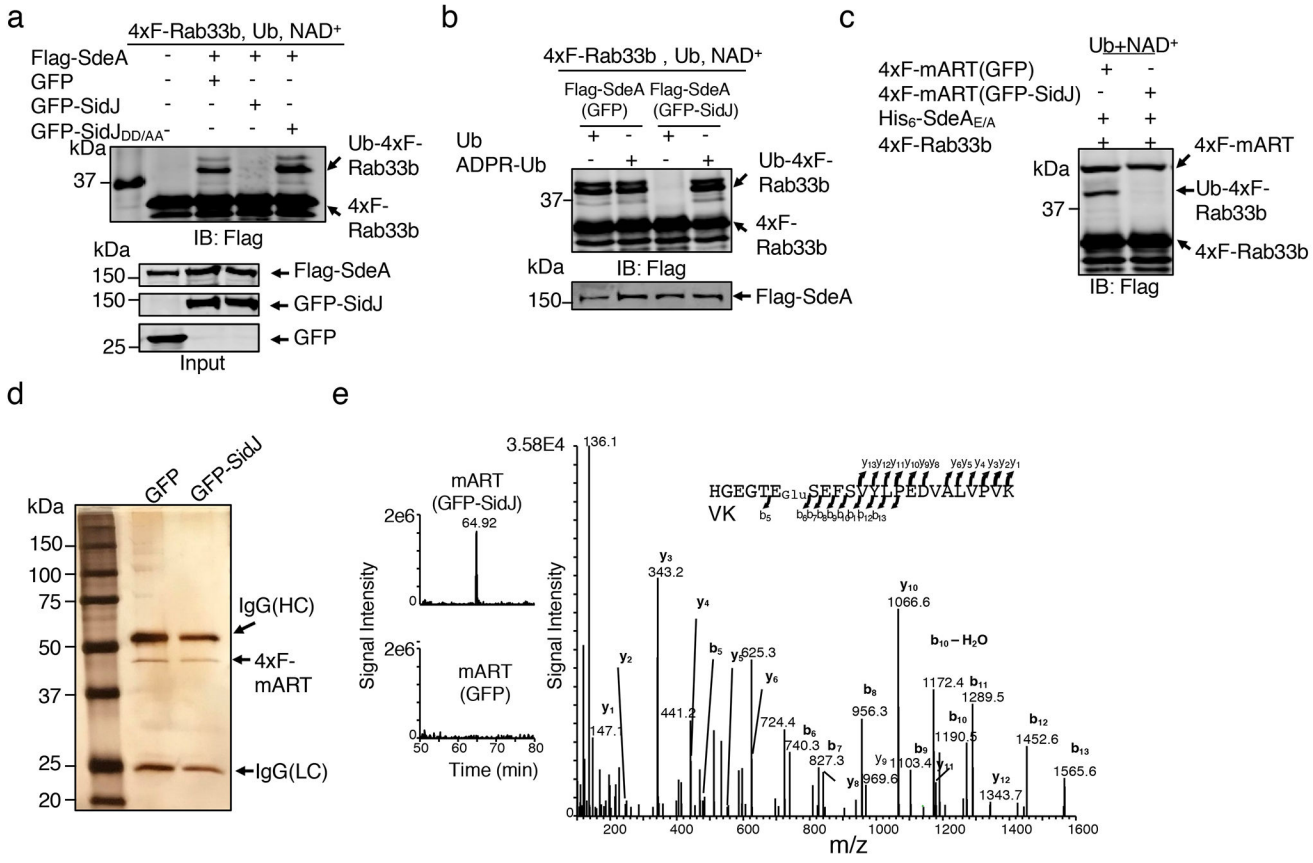

Fig. 2. SidJ post translationally modifies SdeA in mammalian cells and inhibits its activity to catalyze the production of ADP-ribosylated ubiquitin

a. Flag-SdeA coexpressed with SidJ fails to modify Rab33b. Flag-SdeA from HEK293T cells coexpressing relevant proteins was used to ubiquitinate 4xFlag-Rab33b. Ub-Rab33b was detected as described in Fig. 1. $SidJ_{DD/AA}$ is a SidJ mutant defective in suppressing the yeast toxicity of SdeA that carries D542A and D545A mutations.

b. Flag-SdeA coexpressed with SidJ retains the ability to ubiquitinate Rab33b with ADPR-Ub. ADPR-Ub or ubiquitin was incubated with Flag-SdeA purified from HEK293T cells coexpressing GFP or GFP-SidJ. NAD^+ was included in reactions receiving ubiquitin. Rab33b modification was detected with a Flag-specific antibody.

c. SidJ attacks the mART activity of SdeA. 4xFlag-mART ($SdeA_{563-910}$) purified from HEK293T cells coexpressing GFP or GFP-SidJ was incubated with 4xFlag-Rab33b, ubiquitin, NAD^+ and His_6-$SdeA_{E/A}$ for 2 h at 37°C before ubiquitination detection.

d-e. SidJ induces a 129.04 Dalton post-translational modification on E860 of SdeA. Mass spectrometric analysis of 4xFlag-mART* (**d**) identified a posttranslational modification in the fragment -H_{855}GEGTESEFSVYLPEDVALVPVK$_{877-}$ (**e,** left panel). Tandem mass (MS/MS) spectrum shows the fragmentation profile of the modified peptide -H_{855}GEGTE_{Glu}SEFSVYLPEDVALVPVK$_{877-}$, including ions b_5 and b_6 that confirm the modification site at E860 (**e**, right panel). The experiment in each panel was repeated three times with similar results.

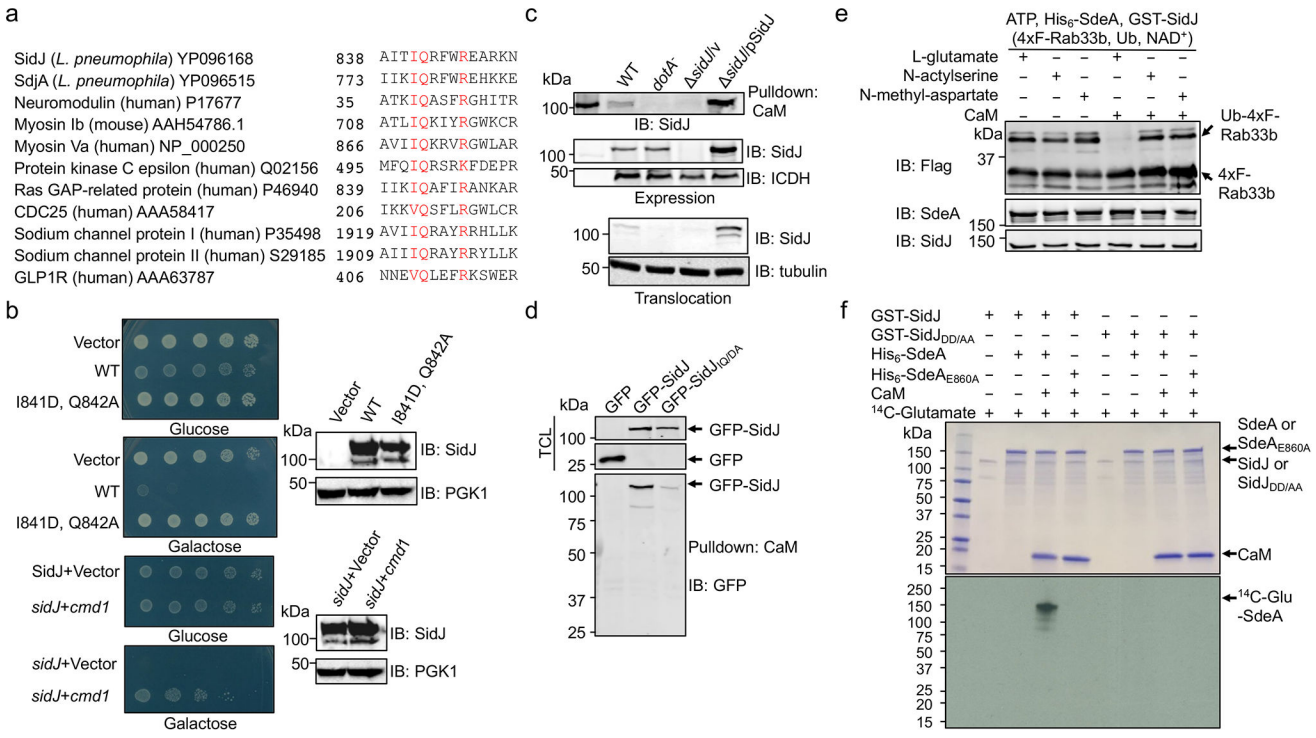

Fig. 3. Calmodulin is the host cofactor required for the glutamylase activity of SidJ

a. SidJ harbors an IQ motif. Alignment of the IQ domain of SidJ and that of several CaM-binding proteins. Conserved residues were highlighted in red. The accession number for each protein was included.

b. The *cmd1* gene suppresses the yeast toxicity of SidJ. **Top two panels**: Images of serially diluted yeast cells inducibly expressing *sidJ* or its IQ mutant spotted onto the indicated media for 2 d. **Lower two panels**: The suppression of SidJ toxicity by *cmd1*. The expression of SidJ in each strain was examined and PGK1 was probed as a loading control (right panels).

c-d. The interactions between SidJ and CaM. Beads coated with CaM were incubated with lysates of macrophages infected with the indicated bacterial strains to probe its binding to SidJ (**c**, top). SidJ in bacteria (**c**, middle) or translocated into the host cytosol (**c**, lower panel) was also examined. The bacterial isocitrate dehydrogenase (ICDH) and tubulin were probed as loading controls, respectively. Lysates of HEK293T cells transfected to express GFP-SidJ or GFP-$SidJ_{IQ/DA}$ were incubated with CaM-coated beads (**d**). SidJ or $SidJ_{IQ/DA}$ bound to CaM was probed by immunoblotting (lower panel). TCL, total cell lysates.

e. Inhibition of SdeA activity by SidJ requires glutamate and CaM. CaM was added to a subset of a series of reactions containing SdeA, GST-SidJ and L-glutamate, N-acetylserine or N-methyl-aspartate. The activity of SdeA was measured by Rab33b ubiquitination.

f. SidJ is a CaM-dependent glutamylase that modifies SdeA at E860. A series of reactions containing the indicated proteins, ^{14}C-glutamate and ATP were allowed to proceed for 2 h at 37°C. The incorporation of ^{14}C-glutamate was detected by autoradiography. Data shown in panels **b-f** were one representative from at least three experiments with similar results.

Author Manuscript Author Manuscript Author Manuscript Author Manuscript

Author Manuscript Author Manuscript Author Manuscript Author Manuscript

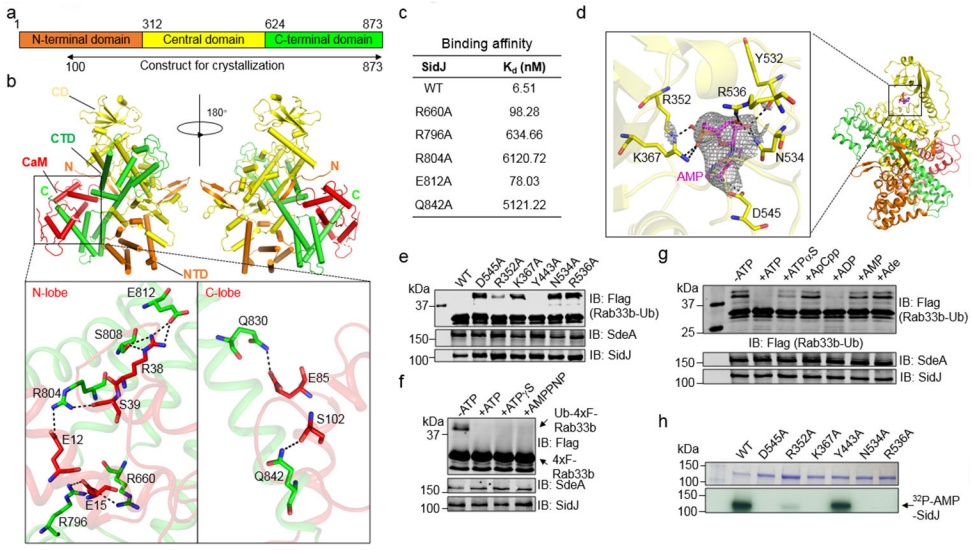

Fig. 4. Structural analysis of the mechanism of SidJ-catalyzed glutamylation

a. Domain organization of SidJ. SidJ consists of the N-terminal domain (orange), the Central domain (yellow) and the C-terminal domain (green).

b. Ribbon diagram representation of the SidJ-CaM complex. In top panels, the N-terminal domain (orange), Central domain (yellow), C-terminal domain (green) of SidJ and CaM (red) are shown. The view on top right is generated by rotating the structure shown on the top left by 180° around the indicated axis. The N and C termini of SidJ are labeled with letters. The missing residues are shown in dashed lines. Lower panels depict interactions between SidJ and the N-lobe/C-lobe of CaM. Residues important for binding are shown in sticks and hydrogen bonds are indicated by dashed lines.

c. Binding of CaM to SidJ and its mutants. The binding affinity was evaluated using microscale thermophoresis. The dissociation constant (K_d) was calculated by the NanoTemper Analysis 2.2.4 software. Data shown were one representative from three experiments with similar results.

d. Ribbon representation of the SidJ-CaM-AMP complex. Key residues of SidJ involved in AMP binding are shown in yellow sticks, AMP is labeled in magenta sticks. Hydrogen bonds are shown as dashed lines. Electron density of an SA (simulated annealing) Fo-Fc omit map for AMP contoured at 3.0 σ.

e. Mutational analysis of residues important for binding AMP. Each SidJ mutant was incubated with SdeA, ATP, L-glutamate and CaM for 2 h before measuring SdeA's ubiquitin ligase activity.

f-g. Activation of SidJ by ATP analogs. The indicated compounds were incubated with SdeA, GST-SidJ, L-glutamate and CaM for 2 h at 37°C before monitoring SdeA's activity in ubiquitinating Rab33b. Note that analogs defective in hydrolysis at the α site cannot activate SidJ.

h. The role of residues important for AMP binding in SidJ self-AMPylation. Each SidJ mutant was incubated with ^{32}P-α-ATP, Mg^{2+} and CaM for 2 h at 37°C and the incorporation of ^{32}P-α-ATP was detected by autoradiography. In panels **c, e-h**, data shown were one representative from at least three independent experiments with similar results.